A coupled model to jointly predict EEG and optical evoked response changes in rats under varying stimulus patterns

Srinivas Laxminarayan*, Gilead Tadmor*, Louis Gagnõn†, David Boas†, Maria Angela Franceschini†, and Dana H. Brooks*
*Department of Electrical and Computer Engineering
Northeastern University, Boston, MA
Email: slaxmina@ece.neu.edu
† Athinoula A. Martinos Center for Biomedical Imaging
Massachusetts General Hospital, Charlestown, MA

***Abstract*—Multimodality functional brain imaging has been gaining importance due to the complementary nature of different imaging modalities. Dynamical systems based models of neural activity and local hemodynamics may offer enhanced spatiotemporal resolution and insight into physiological signals and mechanisms. One major tool for studying brain function is to evoke local responses by repeated application of a stimulus. Under such stimulation neuronal evoked responses show complex habituation to stimuli as the repetition frequency increases beyond 2 Hz. These habituation effects are also reflected in the resulting hemodynamic responses. To understand the relationship between the habituated neural activity and hemodynamics we propose a modeling framework that uses simplified version of an existing neuron model with a control structure enabling habituation prediction and a neurovascular model that captures the relation between neuronal and hemodynamic evoked responses under different stimulus patterns. We report on the accuracy with which this combined model captures the neural and hemodynamic responses across a range of variation in stimulus patterns which includes both frequency and duration variation.**

I. Introduction

In the desire to obtain more information about brain function from non-invasive imaging there has been an increased interest in using multiple noninvasive brain imaging modalities. Perhaps one of the most common combinations measures both electrical response (*e.g.* EEG or MEG) and hemodynamic response (*e.g.* fMRI or diffuse optical measurements) [1], [2]. These modalities complement each other in their spatial and temporal resolution while providing information about functionally connected brain activity. However the question of how to infer brain function efficiently from such multimodal measurements is a current topic of interest. One approach is to attempt to directly correlate the measurements [3]; another, which we follow in the current work, is to postulate dynamical systems based generative, or predictive models, which can simultaneously explain both types of measurements, such as in [4], [5].

A major tool used in systems based modeling approaches for studying brain function is to provoke local "evoked responses" by repeated application of stimuli. It has been known from prior studies of brain function that under repeated stimuli, evoked responses habituate to the stimulus pattern in a complex manner. This habituation is thought to be fundamental to many of the processes that underly learning, memory and cognition [6], [7]. Furthermore this habituation presents a major challenge in using systems based models to combine multimodal data.

Indeed, previous studies of which we are aware using systems based models of concurrent measurements of neural and hemodynamic activity, are only valid under fixed stimulus patterns [5], [8]. These models were not designed to predict the habituation to different stimulus patterns, and hence generalizing them to arbitrary stimulus conditions would involve re-estimation of model parameters to each condition. Here our goal is to contribute to a single generative model capable of predicting both EEG and optical measurements in a fashion that includes predicting the habituation to changes in stimulus application parameters. The model we present here includes an habituation component presented in [9] to predict EEG habituation, and adds to that model prediction of optical measurements via a coupling structure and a hemodynamic model. Fig. 1 summarizes our modeling effort. The input is the stimulus train on the left. The measurements are the EEG and optical measurements on the bottom. The neural mass model includes an habituation control block that automatically modifies its own parameters to predict response to the types of stimulus patterns studied here. The remaining blocks predict the hemodynamic signals derived directly from the optical measurements in a fashion that tracks the changes in those signals that are driven by the changes in the neural mass model output.

The organization of this paper is as follows: Section II describes the experimental procedure and data processing. Section III describes the neuron model outfitted with a habituation prediction control structure. Section IV describes the hemodynamic model and presents a method for reconstruction of its input signals from hemodynamic data. Section V discusses the relation between the neural responses and the inputs of the hemodynamic model. Section VI presents the model performance and validation over all the experimental

978-1-4244-8281-8/11/$26.00 ©2011 IEEE

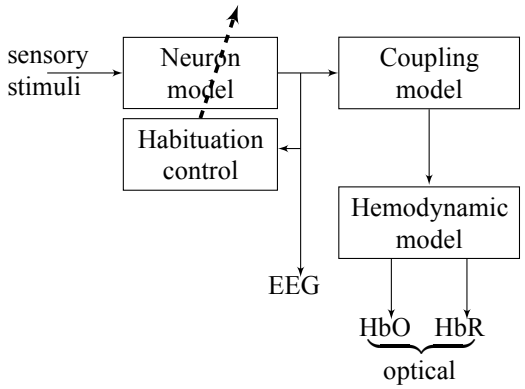

Fig. 1. Sensory stimuli drive the habituation predictive neuron model whose output can be measured by EEG. The Coupling model relates the neuron model output to the inputs of the hemodynamic model which generates oxygenated/de-oxygenated hemoglobin concentration (HbO/HbR). This hemodynamic response can be measured by optical methods.

conditions, and Section VII concludes the paper.

II. Data processing and description

In this section we describe the experimental procedure and data processing in II-A and typical waveforms of the neural and hemodynamic responses in II-B.

A. Experimental procedure

The data were collected by applying a current stimulus at constant amplitude to one fore-paw of rats (medial nerve stimulation), and recording the neural activity using EEG, while monitoring the hemodynamic response using optical measurements at wavelengths of 690 nm and 830 nm. The configuration of the electrodes and optical sources and detectors are shown in Fig. 2.

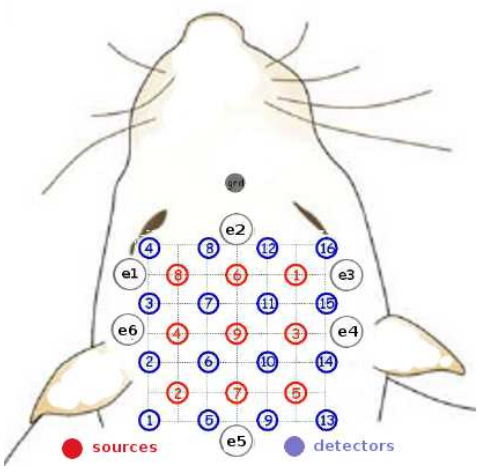

Fig. 2. Illustration of the optical source(red)-detector(blue) cap and EEG electrodes on the rat head. The EEG electrodes e1 and e3 record the neuronal responses from the left/right somatosensory cortex. The 'grd' reference electrode is shown as a gray dot.

The variation of the stimulus pattern, which provoked the variation in response changes we attempt to model, fall into two classes:

1) Stimulus frequency changes: Trains of stimuli were applied for fixed 4-second durations at stimulus frequencies chosen from a random ordering from 1, 2, . . . , 8 Hz. The rest time between the stimulus trains was 12 seconds on average.
2) Stimulus duration changes: Trains of stimuli at a fixed stimulus frequency of 3 Hz were applied for stimulus train durations chosen from a random ordering from 1, 2, . . . , 8 seconds.

Both procedures were repeated 10 times for each fore-paw of each of six rats, resulting in a total of 12 datasets for each class of stimulus variation, or a total of 24. We denote the datasets in the sequel by nS, where n= $\{1,\ldots,6\}$ for frequency experiments, and $\{7,\ldots,12\}$ for duration experiments, and S=$\{$L,R$\}$ to denote the left or right brain region.

We note that the neural response time constants are short and thus the measured EEG should be expected to change rapidly in response to the stimulus frequency changes, while the changes in duration are not expected to have much effect on the EEG. On the other hand, the hemodynamic time constants are longer compared to the stimulus frequency but respond to accumulated metabolic load and thus we would expect some change, mostly in amplitude, with this range of stimulus frequency variation (because the neural response changes and thus the metabolic load does too) and change in both amplitude and duration as a result of the stimulus duration variation.

Before describing the data processing it will be helpful to point out that stimulation of the medial nerve activates the contralateral somatosensory cortex [10] in the brain. Hence the electrodes e1 and e3 (positioned near the somatosensory cortex, as illustrated on Fig. 2) were used for the EEG data, and the source-detector pairs around the somatosensory cortex were used for collecting the optical measurements. The processing of raw data for both sets of measurements are explained briefly:

1) **EEG data:** The raw EEG data were filtered to remove extreme low frequency changes in the baseline and noise from the cardiac cycle and 60 Hz power signal. A nonlinear filtering procedure was followed to improve signal-to-noise ratio, details can be found in [9], and [3].
2) **Optical data:** The measured optical waveforms varied greatly in amplitude across source-detector pairs in an experimentally-dependent manner, due to the exponential attenuation of light in turbid media. Thus the preprocessing for the optical data was somewhat more involved than for EEG, including conversion to hemodynamic quantities, filtering, and selection of useful source-detector pairs.
   - First, temporal changes in the intensity of light were translated into temporal changes in the concentrations of oxy-hemoglobin (ΔHbO) and doxy-hemoglobin (ΔHbR) using the modified Beer Lambert law.

- Second, based on a preliminary study of the calculated hemodynamic signals we determined that the useful signal power was below 3.5 Hz, so an order 10 Hanning FIR low pass filter with a cutoff frequency of 3.5 Hz was applied to the responses.
- Next we needed an objective procedure to identify the useful source-detector pairs. Variations in amplitude and even in amplitude differences prevented the use of a simple amplitude or power threshold, so instead we used a template-based approach designed to identify hemodynamic waveform shapes that corresponded to meaningful physiological responses. In detail, we followed a two-step procedure:
  - The ensemble average of the hemodynamic responses from all source-detector pairs in the somatosensory cortex across all datasets was taken as a representation of a template response waveform.
  - For each dataset the source-detector pairs that on average across all measurements had a correlation coefficient greater than 0.7 with respect to the ensemble average were retained as being representative of the hemodynamic response; the others were discarded. The threshold of 0.7 was chosen as the minimum value so that at least one source-detector pair was retained in each dataset.

  Thus the procedure amounted to a simple heuristic statistical clustering procedure based on waveform shape similarity.

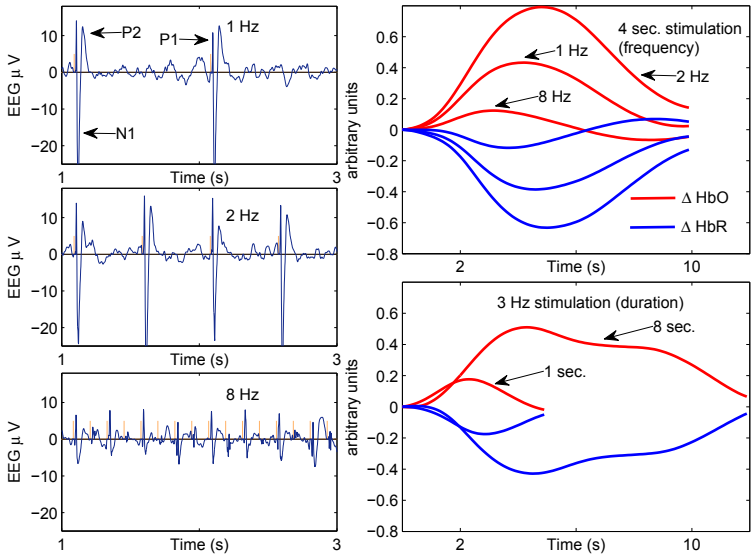

Fig. 3. Left panels: 2 seconds of EEG responses for stimulus frequencies (1,2,8 Hz), for a fixed duration of 4 seconds (dataset 4L). Top right panel: Hemodynamic responses for varying stimulus frequencies. Bottom right panel: Hemodynamic responses for stimulus durations (1,8 seconds) at a fixed frequency of 3 Hz (dataset 7L). No panel is shown for EEG response to duration change since, as noted above, the neural activity response is not sensitive to the duration change.

B. Data description

Typical EEG and hemodynamic responses are shown in Fig. 3. The EEG responses (left panels) are characterized by three distinct "bump-like" segments denoted as P1, N1 and P2. As the stimulus frequency increases the EEG waveshape is roughly stable until 3 Hz, then diminishes significantly in amplitude and at higher frequencies (6-8 Hz) sometimes shows no discernable response to some stimuli. This behavior is the habituation to stimulus frequency that we incorporate into our model via the control block in Fig. 1. As suggested above, the hemodynamic responses reflect the habituation to stimulus by diminishing in amplitude as stimulus frequency increases (top right panel), or responding for extended durations (bottom right panel) when periodic stimuli at 3 Hz are applied for increasing durations.

III. Neuron Model with Habituation Prediction

In this section we briefly discuss the development of a control structure that aids a simplified version of a published neural mass model [11] to predict the habituation to stimulus frequency shown in the EEG responses.

We adopt a recently published neural mass model which was designed to represent the average behavior of synchronized ensemble of neurons [11]. As is typical, the model consists of a Pyramidal Cell (PC) and two InterNeuron (IN) groups, with one acting as a nonlinear feed-forward connection and the other a nonlinear feedback connection. It consists of three input currents, one from the feed-forward connection (I_3^+), one from the thalamus (I_1^+), and one from the surrounding neurons (I_2^+). Our analysis of this model [9] showed that it could be reduced to a second order linear system with three inputs under the conditions represented by the rat EEG data under study with negligible loss of fidelity. Furthermore as a result of this simplification the only parameters of the model which need to vary to match the observed variation in EEG waveforms pertain to the three input currents. Each input current in our reduced-order model has two parameters, its timing with respect to the stimulus, denoted τ_i, and its gain α_i, with $i = \{1, 2, 3\}$. Thus, the entire set of observed EEG responses can be reasonably replicated by the neural mass model by controlling these six parameters.

As illustrated in the left panels of Fig. 3 habituation to stimulus results in diminishing responses (> 2 Hz), and indeed, at a higher stimulus frequencies (> 5 Hz), in some stimulus intervals there are no discernible response waveforms (see the 8 Hz response in Fig. 3). Using a standard approach from nonlinear system identification [12] we developed a control structure, driven by the model output, that changes the model parameters appropriately in order to successfully predict the observed habituation [9]. .

This control is carried out through a control parameter, denoted s, that evolves continuously in time according to a non-linear ODE driven by the rectified model output. This parameter is sampled at the time the next stimulus trigger occurs, denoted by t_s, and its value at that time determines the model parameter for the subsequent response. Thus we

needed to develop both the driving ODE and the mapping from $s(t_s)$ to the model parameters.

The ODE was developed to satisfy the following set of heuristic constraints:

1) A small value of $s(t_s)$ should correspond to the low stimulus frequencies, 1 and 2 Hz, and not change the model parameters.
2) A larger but moderate value of $s(t_s)$ should correspond to the intermediate stimulus frequencies 3, 4, 5 Hz.
3) At high frequencies 6 to 8 Hz $s(t_s)$ should oscillate between moderate and yet larger values as at these frequencies the EEG itself alternates between a diminished but discernible response and no discernible response.

The resulting first-order ODE includes a quadratic time-constant which allows it to satisfy all three constraints.

$$\dot{s} = -\frac{1}{\tau_s}(0.5 + s)s + g_s|y(t)|, \quad \text{with } s(0) = 0, \qquad (1)$$

where τ_s, and g_s were chosen to match the data variation and $y(t)$ is the model output.

To identify the static mappings between s and the parameters of the input currents τ_i and α_i, we simply matched optimized parameter values for each response to corresponding samples of s and fitted continuous functions to model the relationships so discovered. Illustrative scatter plots are shown in Fig. 4. Further details can be found in [9].

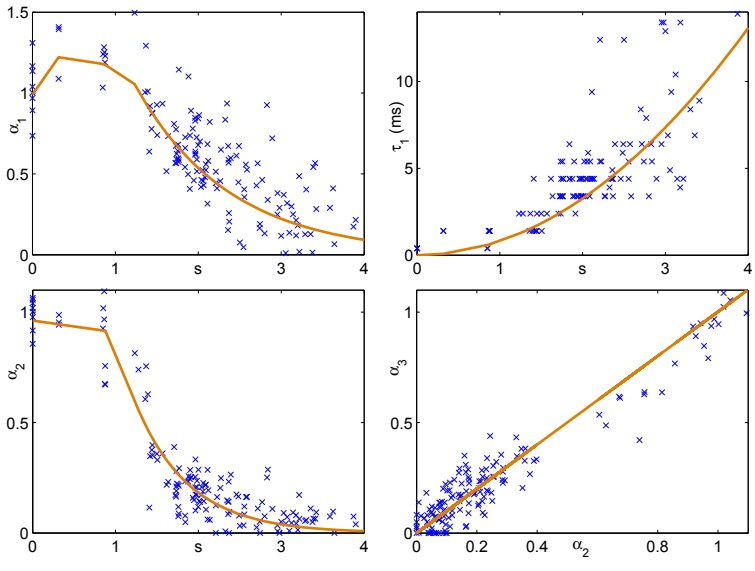

Fig. 4. Scatter plots of the gain parameters α_i, where $i = \{1, 2\}$ vs habituation control parameter s (left panels). The optimized values per response are shown in the scatter plot and the solid curve is the mapping we fit to the scatter. One time parameter, τ_1, vs s (top right), and linear relation between α_2 and α_3 (bottom right), are shown in the same format.

IV. Physiologically Motivated Hemodynamic Model

Our overall strategy to model the relationship between neural activity, for which the EEG is a surrogate, and the hemodynamic quantities estimated from the optical data, is to combine a heuristic coupling model with a physiologically motivated hemodynamic model. To do so we first posit the hemodynamic model, use it to reconstruct appropriate input signals from the hemodynamic signals which are its desired outputs, and then fit the coupling model to produce those inputs for the given EEG signals. In this section we describe the Windkessel hemodynamic model we adopt, as well as the procedure we used to reconstruct its inputs from the hemodynamic estimates..

A. Hemodynamic model

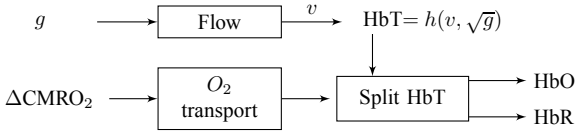

Fig. 5. The block diagram of the single compartment Windkessel model. The total hemoglobin concentration HbT is a function of the vascular volume v, and vascular conductance g. The O_2 transport subsystem, driven by the oxygen demand ΔCMRO_2, provides the time varying weights to split HbT into HbO and HbR.

The hemodynamic model described here is a single compartment model in the class of models based on Windkessel theory[13], [14]. It consists of two subsystems i) blood flow equations, and ii) oxygen transport from blood vessel to tissue. The flow subsystem relates the change in vessel volume to the flow in and out of the vessel, as driven by a change in vascular conductance (g). The O_2 transport subsystem relates the change in partial pressure of O_2 in the vessel to that in the tissue, and is driven by the relevant demand quantity, the variation in cerebral metabolic rate of oxygen (ΔCMRO_2). Fig. 5 shows the block diagram of this model. The model is represented by four nonlinear differential equations, with four states. Of the four states, one state represents the vascular volume v of the flow subsystem, while the other three pertain to the O_2 transport subsystem, specifically the oxygen concentration in the vessel, the number of free oxygen molecules in the tissue, and the oxygen concentration in the pial region that surrounds the vessel.

B. Reconstruction of the hemodynamic model inputs from data

We first focus on reconstructing the vascular conductance g from the hemodynamic data (ΔHbO andΔHbR). The flow subsystem relates g to the vascular volume v. As noted in Fig. 5, the change in total hemoglobin concentration $\Delta\text{HbT}= h(v, \sqrt{g})$. Using the fact that $\Delta\text{HbT}= \Delta\text{HbO}+\Delta\text{HbR}$ and the flow equation we can arrive at a coupled system driven by ΔHbT which generates g and v. Thus, g can be obtained from the data by direct inversion of the flow subsystem.

It turns out that a similar approach cannot be used to reconstruct ΔCMRO_2 because of the nonlinear structure of the O_2 transport subsystem. Instead we transform the problem of reconstructing ΔCMRO_2 into an optimization problem by representing ΔCMRO_2 using a weighted combination of a suitable set of temporal basis functions, and then estimating

the best weights via a least squares fit to the hemodynamic data. For this purpose we chose cubic B-spline basis functions as the basis. For the datasets at hand, a temporal support of 1.5 seconds was suitable. Using this approach the ΔCMRO_2 was reconstructed for all datasets from both set of experiments.

V. Coupling Model

Armed with the reconstructed inputs of the hemodynamic model and the EEG signals from the neural activity, we now describe the development of the coupling model. The first step involves filtering the EEG signals so that the filtered signal has a similar time scale to that of the inputs of the hemodynamic model. A suitable set of temporal basis functions are found for the filtered EEG signals and the inputs of the hemodynamic model. Then, the temporal basis functions on both sides are related via a dynamical system, and the amplitudes at both ends are matched via static mappings. The paragraphs below elaborate the procedure described here.

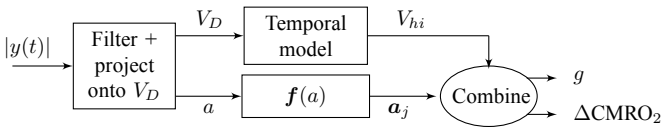

Fig. 6. Block diagram of the coupling model. The rectified EEG response is filtered with a averaging filter. The filtered response is represented by a scalar a and temporal basis function V_D. The temporal model is driven by V_D to generate V_{hi}, where $i = \{1, 2\}$. The static mappings $\boldsymbol{f}(a)$ generate the weights $\boldsymbol{a}_j$, where $j = \{c, g\}$, corresponding to ΔCRMO_2 and g respectively. Linear combination of V_{hi} by the weights $\boldsymbol{a}_j$ generate the signals ΔCMRO_2, and g.

Fig. 6 shows the structure of the coupling model. First, the EEG response is low pass filtered and projected onto the basis function V_D, identified as described below, to obtain the scalar a. Then there are two components, i) a third order linear system driven by V_D to generate the basis functions V_{hi}, where $i = \{1, 2\}$ and, ii) static quadratic mappings from the scalar a to generate the weights $\boldsymbol{a}_j$, where $j = \{c, g\}$, which weigh V_{hi} to form the inputs of the hemodynamic model.

In order to identify the temporal model we required the temporal basis functions for the EEG signals (V_D) and the inputs of the hemodynamic model (V_{hi}, where $i = \{1, 2\}$). We describe the procedure used to obtain V_D, and V_{hi} briefly in the following paragraphs.

As mentioned in Section II-A due to the small time constants of the neural mass the EEG responses are not affected by changes in stimulus duration at a fixed frequency. Thus, we assume that the basis function V_D would be similar for a fixed duration of stimulus irrespective of the stimulus frequency. Hence, we only used the EEG data from duration experiments to find a suitable basis V_D per stimulus duration. The filtered EEG responses from all duration datasets (7L to 12R) per stimulus duration was collected into a matrix where rows correspond to the number of datasets and columns, the time points. Performing an SVD of this matrix we obtain V_D which is the temporal basis corresponding to the dominant singular value that captured $> 93\%$ of the variation. This process is repeated for each stimulus duration.

To obtain V_{hi} the inputs of the hemodynamic model were reconstructed from the data as described in Section IV-B for all duration datasets (7L to 12R) and collected into a matrix for each stimulus duration. An SVD of this matrix revealed that the top two dominant singular values captured $> 90\%$ of the variations in the reconstructed inputs. Hence, we chose the corresponding temporal basis functions to be V_{hi}, where $i = \{1, 2\}$ for each stimulus duration.

The temporal model was then identified by postulating a 3rd order linear system structure and estimating its parameters via nonlinear least squares so as to minimize the error between V_{hi} obtained from the procedure described above, and the output of the system driven by V_D over all stimulus durations.

The static mappings relate a to $\boldsymbol{a}_j$, where $j = \{c, g\}$. The scalar a were obtained by projecting a filtered EEG response onto V_D for a given dataset. Similarly, $\boldsymbol{a}_j$ were obtained by projecting ΔCMRO_2 and g onto V_{hi} for the same dataset. A quadratic polynomial whose coefficients were estimated using least squares was found to be suitable to relate a to $\boldsymbol{a}_j$.

VI. Results

In this section we present the performance of the generative model across all datasets from both sets of experiments.

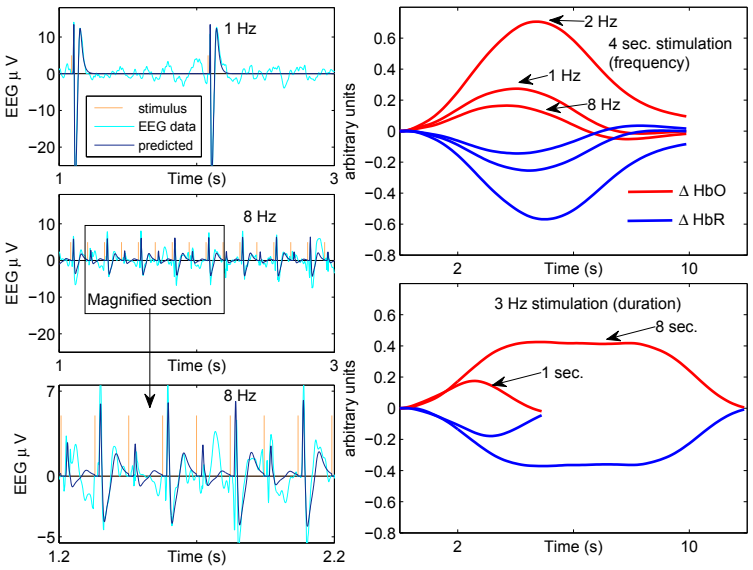

Fig. 7. The coupled model predicting the 1Hz and 8Hz EEG and hemodynamic data shown in Fig. 3. The true EEG data is plotted in light color, and the model prediction in a dark color. 8 Hz response is magnified in the bottom panel to show that the model captures the features of the habituation of the P1-N1-P2 waveform to stimulus. The right hand panels show the model prediction of the hemodynamic responses corresponding to those in Fig. 3.

We illustrate our results with a sample result (Fig. 7) using the model to predict the 1 Hz and 8 Hz EEG and hemodynamic responses shown in Fig. 3. The features of the habituation of the P1-N1-P2 waveform are captured by the predicted EEG (see the middle and bottom left panels) even for the

most challenging (8 Hz stimulus) case. The predicted EEG then drives the other subsystems in Fig. 1 to generate the hemodynamic responses.

TABLE I
FEATURES FROM THE PREDICTED EEG ARE COMPARED TO EEG DATASETS FROM ALL FREQUENCY EXPERIMENTS.

Feature	Best	LTOCV
PT	0.69 ± 1.95 ms	0.81 ± 1.85 ms
NT	-0.32 ± 2.78 ms	-0.38 ± 2.91 ms
P2T	-3.55 ± 7.83 ms	-3.91 ± 6.84 ms
PP	0.05	0.10
NP	0.05	0.08
P2A	0.22	0.26

For characterizing the performance of the predictive neural mass model (presented in Section III) we extracted several relevant features from the EEG data in the frequency experiments. The features are i) P1 peak amplitude (PP), ii) P1 peak time (PT), iii) N1 peak amplitude (NP), iv) N1 peak time (NT), v) P2 start time (P2T), and vi) P2 area (P2A). Table I reports the error in the three time features (PT, NT, and P2T) in ms, and the mean relative error (using the l2 norm) in the shape features (PP, NP, and P2A), with respect to features extracted from all the datasets. The table also presents overall Leave Two Out Cross Validation (LTOCV) results across the datasets. The LTOCV procedure involves leaving out both the datasets corresponding to the left and right half brains of the chosen rat, estimating the model and computing the error when tested on the datasets from the left-out rat.

TABLE II
THE MEAN PERFORMANCE METRIC E BETWEEN THE GENERATED HEMODYNAMIC RESPONSES AND THE DATA OVER ALL DATASETS FROM BOTH SET OF EXPERIMENTS.

Experiment	Best	LTOCV
Frequency	0.017	0.047
Duration	0.012	0.028

The EEG signals predicted by the neural mass model then drive the coupling and hemodynamic models discussed in Sects. IV, and V to generate the hemodynamic responses. Table II reports on the mean performance of the coupled model using the performance metric

$$E = \frac{\text{Estimation error of the model}}{\text{Standard deviation of the data}} - 1,$$

over the hemodynamic data from all frequency and duration experiments. The estimation error of the model comprises of two terms, i) the standard deviation of the data, and ii) the model mismatch which is the norm of the difference between the model output and the sample mean of the data. Thus, the metric $E = 0$ when the model output matches the sample mean of the data, and $E > 0$ if there is a mismatch. The table also reports the metric E for model validation by using the LTOCV method.

Tables I, and II show that the generative model captures the essential characteristics of the neuronal and hemodynamic evoked responses under both stimulus patterns.

VII. CONCLUSION

In this paper we presented a single generative model that can jointly predict evoked EEG and the related hemodynamic responses under habituation to stimulus frequency and duration. The model was obtained by enabling a mass neuron model to predict the habituation to stimulus, relating the predicted neural responses to the inputs of a hemodynamic model via a coupling model, and finally generating the hemodynamic responses. The result tables suggest that the generative model captures the essential features of evoked responses under habituation to variations in stimulus frequency and duration.

ACKNOWLEDGMENT

The authors would like to thank Ilkka Nissila and Weicheng Wu, for collecting the data. This work was supported in part by the Bernard M. Gordon Center for Subsurface Sensing and Imaging Systems (Gordon-CenSSIS) under the Engineering Research Centers Program of the National Science Foundation (NSF) (award EEC-9986821), and by RO1EB001954.

REFERENCES

[1] B. Horwitz and D. Poeppel, "How can EEG/MEG and fMRI/PET data be combined?" *Hum. Brain Mapp.*, vol. 17, no. 1, pp. 1–3, 2002.
[2] J. Riera, E. Aubert, K. Iwata, R. Kawashima, X. Wan, and T. Ozaki, "Fusing EEG and fMRI based on a bottom-up model: inferring activation and effective connectivity in neural masses." *Phil. Trans. Roy. Soc. B*, vol. 360, pp. 1025–1041, May 2005.
[3] M. A. Franceschini, I. Nissil, W. Wu, S. G. Diamond, G. Bonmassar, and D. Boas, "Coupling between somatosensory evoked potentials and hemodynamic response in the rat." *Neuroimage.*, vol. 41, no. 2, pp. 189–203, 2008.
[4] B. Rosengarten, H. Lutz, and K. A.Hossmann, "A control system approach for evaluating somatosensory activation by laser-doppler flowmetry in the rat cortex," *Jrnl. Neurosci. methods*, vol. 130, pp. 75–81, 2003.
[5] R. C. Sotero and N. J. Trujillo-Barreto, "Biophysical model for integrating neuronal activity, EEG, fMRI and metabolism." *Neuroimage*, vol. 39, pp. 290–309, 2008.
[6] A. S. Bristol and T. J. Carew, "Differential role of inhibition in habituation of two independent afferent pathways to a common motor output," *Learn. Memory*, vol. 12, pp. 52 – 60, 2005.
[7] Y. Noguchi, K. Inui, and R. Kakigi, "Temporal Dynamics of Neural Adaptation Effect in the Human Visual Ventral Stream." *Jrnl. of Neurosci.*, vol. 24, no. 28, pp. 6283–6290, Jul. 14 2004.
[8] J. J. Riera, W. Xiaohong, J. C. Jimenez, R. Kawashima, and T. Ozaki, "Nonlinear local electrovascular coupling. II: From data to neuronal masses." *Human Brain Mapping*, vol. 28, no. 4, pp. 335–354, 2007.
[9] S. Laxminarayan, G. Tadmor, M. A. Franceschini, S. G. Diamond, E. Miller, and D. H. Brooks, "Modeling habituation in rat EEG evoked responses via a neural mass model with feedback." *Biological cybernetics*, under review.
[10] S. C. Bhatnagar, *Neuroscience for the Study of Communicative Disorders*. Lippincott Williams and Wilkins, 2002.
[11] J. J. Riera, W. Xiaohong, J. C. Jimenez, and R. Kawashima, "Nonlinear local electrovascular coupling. I: A theoretical model." *Human Brain Mapping*, vol. 27, no. 11, pp. 896–914, 2006.
[12] O. Nelles, *Nonlinear system identification.* Springer, 2000.
[13] J. Mandeville, J. Marota, C. Ayata, G. Zaharchuk, M. Moskowitz, B. Rosen, and R. Weisskoff, "Evidence of a cerebrovascular postarteriole windkessel with delayed compliance." *Jrnl of Cereb. Blood Flow and Metab.*, vol. 19, no. 6, pp. 679–689, 1999.
[14] R. Buxton, E. Wong, and L. Frank, "Dynamics of blood flow and oxygenation changes during brain activation: The balloon model." *Magnetic resonance in med.*, vol. 39, pp. 855–864, 1998.